

November 07, 2011

## Electrostatic tuning of ferromagnetic resonance and magnetoelectric interactions in ferrite-piezoelectric heterostructures grown by chemical vapor deposition

Ning Li

*University of Alabama - Tuscaloosa*

Ming Liu

*Northeastern University*

Ziyao Zhou

*Northeastern University*

Nian X. Sun

*Northeastern University*

D. V. B. Murthy

*Northeastern University*

*See next page for additional authors*

---

### Recommended Citation

Li, Ning; Liu, Ming; Zhou, Ziyao; Sun, Nian X.; Murthy, D. V. B.; Srinivasan, Gopalan; Klein, Tonya M.; Petrov, Vladimir M.; and Gupta, Arunava, "Electrostatic tuning of ferromagnetic resonance and magnetoelectric interactions in ferrite-piezoelectric heterostructures grown by chemical vapor deposition" (2011). *Electrical and Computer Engineering Faculty Publications*. Paper 139. <http://hdl.handle.net/2047/d20002345>

---

**Author(s)**

Ning Li, Ming Liu, Ziyao Zhou, Nian X. Sun, D. V. B. Murthy, Gopalan Srinivasan, Tonya M. Klein, Vladimir M. Petrov, and Arunava Gupta

## Electrostatic tuning of ferromagnetic resonance and magnetoelectric interactions in ferrite-piezoelectric heterostructures grown by chemical vapor deposition

Ning Li, Ming Liu, Ziyao Zhou, Nian X. Sun, D. V. B. Murthy et al.

Citation: *Appl. Phys. Lett.* **99**, 192502 (2011); doi: 10.1063/1.3658900

View online: <http://dx.doi.org/10.1063/1.3658900>

View Table of Contents: <http://apl.aip.org/resource/1/APPLAB/v99/i19>

Published by the [American Institute of Physics](http://www.aip.org).

---

### Related Articles

Magnetoelectric manipulation of domain wall configuration in thin film Ni/[Pb(Mn<sub>1/3</sub>Nb<sub>2/3</sub>)O<sub>3</sub>]<sub>0.68</sub>-[PbTiO<sub>3</sub>]<sub>0.32</sub> (001) heterostructure

*Appl. Phys. Lett.* **100**, 092902 (2012)

Effect of site-disorder on magnetism and magneto-structural coupling in gallium ferrite: A first-principles study

*J. Appl. Phys.* **111**, 043915 (2012)

Multiferroic response of nanocrystalline lithium niobate

*J. Appl. Phys.* **111**, 07D907 (2012)

Field-induced continuous rotation of the polarization in multiferroic Mn<sub>0.95</sub>Co<sub>0.05</sub>WO<sub>4</sub>

*J. Appl. Phys.* **111**, 07D903 (2012)

Anisotropic bimodal distribution of blocking temperature with multiferroic BiFeO<sub>3</sub> epitaxial thin films

*Appl. Phys. Lett.* **100**, 072402 (2012)

---

### Additional information on *Appl. Phys. Lett.*

Journal Homepage: <http://apl.aip.org/>

Journal Information: [http://apl.aip.org/about/about\\_the\\_journal](http://apl.aip.org/about/about_the_journal)

Top downloads: [http://apl.aip.org/features/most\\_downloaded](http://apl.aip.org/features/most_downloaded)

Information for Authors: <http://apl.aip.org/authors>

## ADVERTISEMENT



# Electrostatic tuning of ferromagnetic resonance and magnetoelectric interactions in ferrite-piezoelectric heterostructures grown by chemical vapor deposition

Ning Li,<sup>1</sup> Ming Liu,<sup>2</sup> Ziyao Zhou,<sup>2</sup> Nian X. Sun,<sup>2</sup> D. V. B. Murthy,<sup>3</sup> Gopalan Srinivasan,<sup>3</sup> Tonya M. Klein,<sup>1</sup> Vladimir M. Petrov,<sup>3</sup> and Arunava Gupta<sup>1,a)</sup>

<sup>1</sup>Center for Materials for Information Technology, University of Alabama, Tuscaloosa, Alabama 35487, USA

<sup>2</sup>Department of Electrical and Computer Engineering, Northeastern University, Boston, Massachusetts 02115, USA

<sup>3</sup>Physics Department, Oakland University, Rochester, Michigan 48309, USA

(Received 21 July 2011; accepted 9 October 2011; published online 7 November 2011)

Magnetoelectric interactions as a function of applied electric field have been studied in ferrite-ferroelectric heterostructures at microwave frequencies. The measurements are performed on 1.5–2.0  $\mu\text{m}$  thick nickel ferrite ( $\text{NiFe}_2\text{O}_4$ ) films grown heteroepitaxially on lead zinc niobate-lead titanate and lead magnesium niobate-lead titanate substrates using direct liquid injection chemical vapor deposition. Large shifts in the ferromagnetic resonance profile are observed in these heterostructures due to strong magnetoelectric coupling resulting from electrostatic field induced changes in the magnetic anisotropy field. Theoretical estimates of field shifts are in good agreement with the experimental data. © 2011 American Institute of Physics. [doi:10.1063/1.3658900]

Multiferroic composites of ferromagnetic and ferroelectric materials are important for studies on electric-and-magnetic subsystem couplings mediated by mechanical forces, which are of considerable interest for future device applications.<sup>1–3</sup> The nature of direct magnetoelectric (ME) effect in the composites is studied by application of a magnetic field that produces a mechanical strain, resulting in an induced polarization.<sup>1</sup> For the converse ME effect, one studies the magnetic response of the sample to an applied electric field.<sup>4</sup> Several ferromagnetic-piezoelectric composites are reported to exhibit strong direct or converse ME effects.<sup>1–4</sup> Resonance enhancement of the ME coupling at bending resonance or electromechanical resonance (EMR) corresponding to acoustic modes has also been observed.<sup>2</sup> This work focuses on converse ME effects by electrostatic tuning of ferromagnetic resonance (FMR) in ferrite-ferroelectric composites.<sup>5–13</sup> The piezoelectric strain due to an electric field  $E$  manifests as an internal magnetic field in the ferromagnetic phase that causes a frequency shift  $\Delta f$  or a field shift  $\Delta H$  in the FMR or hybrid modes, with the strength of ME interaction  $A$  defined by  $A = \Delta f/E$  (or  $\Delta H/E$ ). Earlier studies of this type primarily focused on epoxy bonded layered composites<sup>5–8</sup> or polycrystalline ferromagnetic films deposited on ferroelectric substrates.<sup>9–15</sup>

Herein, we report on the converse ME effect in heteroepitaxial structures of nickel ferrite  $\text{NiFe}_2\text{O}_4$  (NFO) films directly grown onto (001)-oriented single crystal lead zinc niobate-lead titanate (PZN-PT) or lead magnesium niobate-lead titanate (PMN-PT) substrates. Based on our previous theoretical work, a strong ME effect is expected in such structures because of the strong coupling resulting from high values of the magnetostriction and piezoelectric coefficients.<sup>5</sup> The strain-mediated coupling is expected to be stronger in such epitaxial lattice-matched heterostructures that are free of any foreign medium at the interface, as in epoxy

bonded bilayers, or even in polycrystalline films deposited directly on piezoelectric substrates.

The nickel ferrite films were deposited on PZN-PT and PMN-PT substrates by direct liquid injection-chemical vapor deposition (DLI-CVD) using a Brooks Instrument DLI 200 vaporizer system. Anhydrous  $\text{Ni}(\text{acac})_2$  and  $\text{Fe}(\text{acac})_3$  (acac = acetylacetonate) in the molar ratio of 1:2 were used as precursor sources dissolved in  $N,N$ -dimethylformamide for the DLI vaporizer system using argon as the carrier gas.<sup>16</sup> The vaporized mixture was combined with a flow of preheated oxygen gas prior to introduction into the CVD reactor. Films were deposited at substrate temperatures of 600 and 700 °C with thicknesses in the range of 1.5–2.0  $\mu\text{m}$ . Energy-dispersive x-ray spectroscopy (EDS) confirmed that nearly stoichiometric films ( $\text{Fe}:\text{Ni} = 2.05\text{--}2.10$ ) were obtained at both growth temperatures.

A standard x-ray diffraction setup (Phillips X'pert Pro) was used to determine the phase and epitaxy of the films. Large-angle  $\theta$ - $2\theta$  scans ( $2\theta$  from 10° to 110°) showed only diffraction peaks corresponding to the (00 $l$ ) planes of NFO film and the substrate. No evidence of any secondary phases or misoriented grains was found from the x-ray measurements. Figures 1(a) and 1(b) show  $\theta$ - $2\theta$  plots around the (004) peak for NFO films on PMN-PT and PZN-PT, respectively, grown at 700 °C. The calculated lattice parameters are close to the bulk value (0.834 nm) suggesting that the films are essentially completely relaxed. The full width at half maximum (FWHM) values of omega scans of (004) reflection of NFO films grown on PMN-PT and PZN-PT are 0.27° and 0.33°, respectively, as shown in the insets. As an indication of degree of out-of-plane texture of epitaxial NFO films, these FWHM values are only about double of those for the substrates (0.14° and 0.17°). Epitaxy of films grown both at 600 and 700 °C was confirmed from  $\varphi$  scans of the  $\text{NiFe}_2\text{O}_4$  {202} planes, which showed the expected four-fold cubic symmetry of the spinel structure aligned with the crystal axes of the substrate. The  $\varphi$  scan results for both the film and

<sup>a)</sup>Electronic mail: agupta@mint.ua.edu.

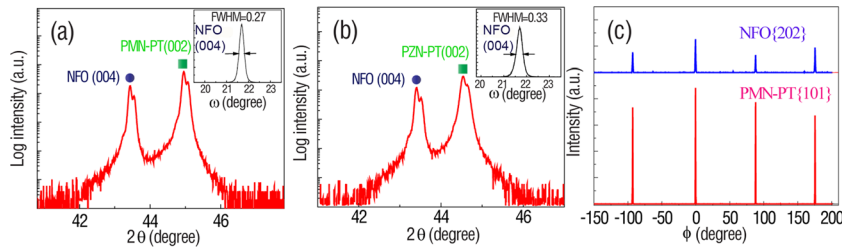


FIG. 1. (Color online) Normal  $\theta$ - $2\theta$  x-ray diffraction patterns for heteroepitaxial NFO films grown on (001)-oriented (a) PMN-PT and (b) PZN-PT substrate. Only the scan range around the (004) peak for the respective films are shown in the plots. The omega scans of the NFO (004) diffraction peak on the two substrates are shown as insets. (c) Phi scans showing the four-fold symmetry and overlap of the {101} peaks of the PMN-PT substrate and {202} peaks of NFO film indicating cube-on-cube epitaxy.

the substrate in the case of NFO film grown on PMN-PT at  $700^\circ\text{C}$  are shown in Fig. 1(c).

The surface morphology and microstructure of NFO films were examined by atomic force microscopy (AFM) and high resolution transmission electron microscopy (HRTEM). Unlike NFO films grown on  $\text{MgAl}_2\text{O}_4$  and  $\text{MgO}$  substrates that are atomically smooth ( $\text{rms} < 0.5\text{ nm}$ ) even for thickness  $> 1\ \mu\text{m}$ ,<sup>16</sup> the roughness increases with increasing film thickness on PZN-PT and PMN-PT substrates, with roughness in the range of 20-30 nm for the films studied. HRTEM study confirmed epitaxial growth of the films on both substrates, but also indicated the presence of dislocations and anti-phase boundaries in the films, which may contribute to increased FMR line-width. The details of the study will be published separately.

ME interactions of the epitaxial NFO/PMN-PT and NFO/PZN-PT were investigated by obtaining FMR profiles at frequencies of 6–11 GHz as a function of applied electric field. An S-shaped coplanar waveguide was used to perform the FMR measurements. Additionally, an external DC magnetic field was applied in the film plane along the [100] or [110] direction of NFO. Representative data for a sample of  $1.5\ \mu\text{m}$  thick NFO on PZN-PT grown at  $700^\circ\text{C}$  are shown in Fig. 2. For  $E = 0$ , the peak-to-peak line-width  $\Delta H_{pp} = 670\text{ Oe}$  is smaller than  $\Delta H_{pp} = 850\text{ Oe}$  for films grown at  $600^\circ\text{C}$ . Assuming  $g = 2.2$  (gyromagnetic ratio  $\gamma \approx 3.1\text{ GHz/kOe}$ ), the effective magnetization  $4\pi M_{\text{eff}} = 4\pi M_s + H_a$ , where  $H_a$  is the anisotropy field, is estimated from the FMR profile in Fig. 2 to be 3.1 kG. Using  $H_a = -112\text{ G}$  (Ref. 17) for bulk single crystal NFO, one obtains  $4\pi M_s = 3.2\text{ kG}$ , which is in very good agreement with measured values.<sup>17</sup> Similar FMR characteristics were observed for heteroepitaxial NFO films grown on (001) PMN-PT substrates.

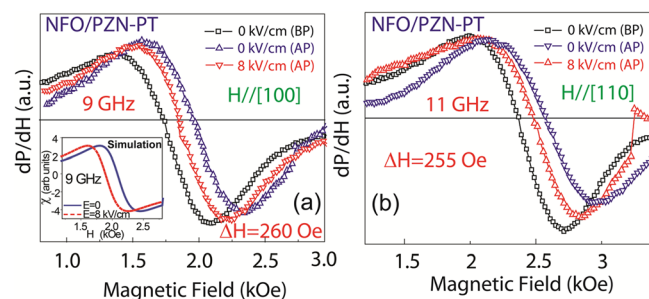


FIG. 2. (Color online) Ferromagnetic resonance absorption spectra as a function of external magnetic field measured with and without applied external electric field. (a)  $\text{NiFe}_2\text{O}_4/\text{PZN-PT}$  heteroepitaxial structure measured at 9 GHz with magnetic field along [100] direction; (b) same heteroepitaxial structure as in (a) measured at 11 GHz with magnetic field along [110] direction. The terms “BP” and “AP” correspond to “before poling” and “after poling,” respectively. The inset in (a) shows simulated FMR profiles at 9 GHz using effective demagnetization factor method.

Upon application of an electric field ( $E$ ) across the NFO/PZN-PT substrate, a shift in the NFO FMR profiles is observed, as shown in Fig. 2. A similar shift is also observed for NFO deposited on PMN-PT substrates. The DC electric field applied across the PZN-PT or PMN-PT substrate results in an in-plane isotropic strain caused by the inverse piezoelectric effect. Given the high temperature growth of NFO on PZN-PT (PMN-PT), the substrate undergoes a cubic to rhombohedral structural transition when the samples are cooled down to room temperature. Consequently, the PZN-PT (PMN-PT) develops a multiple ferroelectric domain structure with a random distribution of the spontaneous polarization. By poling such epitaxial structures with an electric field of  $5\text{ kV/cm}$ , a large irreversible remanent stress is produced in-plane with well-aligned domain structure. As shown in Fig. 2, remarkable shifts of the FMR spectra at both 9 and 11 GHz are produced by poling the epitaxial NFO/PZN-PT structure. The resonance field shifts arising from this poling-induced stress are  $\Delta H = 260$  and  $255\text{ Oe}$  at 9 and 11 GHz, respectively, indicating that poling-induced remanent magnetic anisotropy favors making the in-plane magnetization process harder. However, on subsequent application of an electric field,  $E = 8\text{ kV/cm}$ , the resonance field is reduced by 130 and  $125\text{ Oe}$  for the [110] and [100] directions, respectively, indicating that the epitaxial NFO film experiences an opposite strain or stress in comparison with that experienced during the poling process. Moreover, no significant  $E$  field-induced FMR line-width change is observed, indicating the creation of homogenous  $E$ -induced magnetic anisotropy. Thus, we estimate the ME coefficient  $A = \Delta H/E \approx 16\text{ Oe cm/kV}$  based on the measured resonance fields for  $E = 0$  and  $8\text{ kV/cm}$  for poled samples at 9 and 11 GHz.

The nature of static  $E$ -tuning of magnetic parameters of the NFO/PZN-PT heteroepitaxial structure was also studied by electric-field induced changes in the magnetic hysteresis loops, which were carried out using a vibrating sample magnetometer (VSM). Figure 3 shows  $E$ -dependence of  $M$  vs.  $H$  for  $H$  applied along the [100] and [110] direction of NFO/PZN-PT, respectively. Both of them display an  $E$ -induced easy magnetization process which is consistent with the observation in  $E$ -induced FMR shift. The fractional remanent magnetization change  $\Delta M/M(E=0) = [M(E) - M(E=0)]/M(E=0)$  reaches 15% with  $E = 8\text{ kV/cm}$  applied across PZN-PT. Assuming  $4\pi M_s = 3.2\text{ kG}$ ,<sup>17</sup> and for  $M(E=0)/M_s = 0.3$  based on hysteresis data in Fig. 3, we obtain an ME coupling coefficient of  $A = \Delta M/E = 18\text{ Oe cm/kV}$ , which is in very good agreement with  $A$  obtained from static  $E$ -field tuning FMR data in Fig. 2.

Next, we provide theoretical estimates of the ME coefficient  $A$  for comparison with the observed results. We have

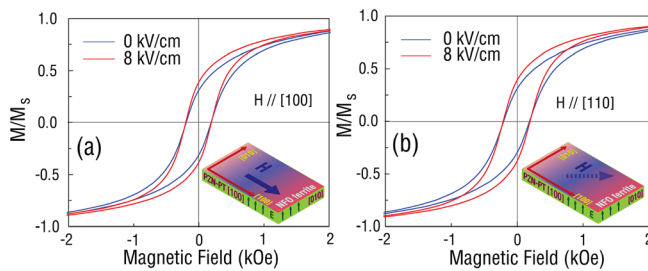


FIG. 3. (Color online) Magnetic hysteresis loops and remanence changes with electric field for the  $\text{NiFe}_2\text{O}_4/\text{PZN-PT}$  heteroepitaxial structure with the external magnetic field along: (a) [100] direction and (b) [110] direction.

used the effective demagnetization factor method to solve the equation of motion of magnetization and obtained FMR profiles of absorption versus  $H$  for a series of  $E$  values. The results for  $E = 0$  and  $8 \text{ kV/cm}$  are shown in the inset of Fig. 2(a) for comparison with the experimental data. Demagnetization factors due to sample geometry, magnetocrystalline anisotropy, and electric field-induced stress (i.e., due to the ME effect) are considered for the calculation. Using the theory described in Ref. 18 and the following parameters for NFO:  $4\pi M_s = 3.2 \text{ kG}$ , anisotropy field  $H_a = -112 \text{ G}$ , and elastic compliance  $c_{11} = 22 \times 10^{10} \text{ N/m}^2$  and for PZN-PT poled along [011]:  $d_{31} = -3000 \text{ pm/V}$ ,  $d_{32} = 1100 \text{ pm/V}$ ,  $c_{11} = 6.7 \times 10^{10} \text{ N/m}^2$ , we obtain a field shift of  $190 \text{ Oe}$  and  $A = 23.8 \text{ Oe cm/kV}$ . Thus, there is a good agreement between theory and experimental data. A more rigorous theory that is also applicable for epitaxially strained thin films due to lattice mismatch is provided in Ref. 19.

The coefficient  $A$  for the heteroepitaxial structure is about a factor of 4 higher than for a bilayer of  $0.1 \text{ mm}$  thick NFO epoxy bonded to  $0.5 \text{ mm}$  thick PZN-PT.<sup>20</sup> The theory predicts an increase in  $A$  with increasing value of the magnetostriction coefficient  $\lambda$ . Thus, one anticipates a much lower  $A$  in bilayers with yttrium iron garnet (YIG) ( $\lambda = 2 \text{ ppm}$ ) or barium hexaferrite (BaM) ( $\lambda = 8 \text{ ppm}$ ) as compared to samples with NFO ( $\lambda = 30 \text{ ppm}$ ). Indeed, the ME coefficient measured for NFO/PMN-PT in this study is a factor of 10-20 higher than for YIG/PMN-PT (Ref. 5) and for bonded BaM/PZT or BaM/BST heterostructures.<sup>14</sup>

The epitaxial structures studied here are of interest for electric field tunable microwave devices such as resonators, band-pass filters, phase shifters, and delay lines.<sup>7</sup> The attractive feature in all these devices is the electric field or voltage tunability of a ferrite device. Magnetic field tuning of ferrite devices is often slow, noisy, and requires kW power for operation and the devices cannot be miniaturized or integrated with semiconductor processing technology. In contrast, electric field tuning can be rapid, less noisy, requires minimal power and the devices can be miniaturized. For device applications, however, it is necessary to grow epitaxial

NFO films with even lower FMR line-widths than the values reported here.

In summary, large electric field tuning of magnetic properties has been observed due to ME interactions in chemical vapor deposited heteroepitaxial  $\text{NiFe}_2\text{O}_4/\text{PZN-PT}$  and  $\text{NiFe}_2\text{O}_4/\text{PMN-PT}$  multiferroic composites. With application of an electrostatic field of  $8 \text{ kV/cm}$ , ferromagnetic resonance field shifts of  $125\text{--}130 \text{ Oe}$  are observed, corresponding to ME coefficient  $A \approx 16 \text{ Oe cm/kV}$ . The calculated value of  $A$  is consistent with observed changes in remanent magnetization in the hysteresis loops with static  $E$ -tuning and also with theoretical estimates. Efforts are underway to reduce the FMR line-width of NFO films to a value closer to those observed in bulk single crystals ( $\sim 50\text{--}100 \text{ Oe}$ )<sup>17</sup> in order to realize robust electric field-tunable microwave devices.

We are grateful to Y.-H. A. Wang for help with initial set up of the DLI-CVD system and T. Mewes for use of his system in obtaining preliminary FMR measurements. This work was supported by grants from the Office of Naval Research (Grant No. N00014-09-0119, Dr. Daniel Green) and the Army Research Office.

- <sup>1</sup>C.-W. Nan, M. I. Bichurin, S. Dong, D. Viehland, and G. Srinivasan, *J. Appl. Phys.* **103**, 031101 (2008).
- <sup>2</sup>S. Priya, R. Islam, S. Dong, and D. Viehland, *J. Electroceram.* **19**, 149 (2007).
- <sup>3</sup>G. Srinivasan, *Ann. Rev. Mater. Res.* **40**, 153 (2010).
- <sup>4</sup>W. Eerenstein, M. Wiora, J. L. Prieto, J. F. Scott, and N. D. Mathur, *Nature Mater.* **6**, 348 (2007).
- <sup>5</sup>S. Shastry, G. Srinivasan, M. I. Bichurin, V. M. Petrov, and A. S. Tatarenko, *Phys. Rev. B.* **70**, 064416 (2004).
- <sup>6</sup>A. Semenov, S. F. Karmanenko, B. A. Kalinikos, G. Srinivasan, A. N. Slavin, and J. V. Mantese, *Electron. Lett.* **42**, 641 (2006).
- <sup>7</sup>G. Srinivasan and Y. K. Fetisov, *Integr. Ferroelectr.* **83**, 89 (2006).
- <sup>8</sup>Y. K. Fetisov and G. Srinivasan, *Appl. Phys. Lett.* **88**, 143503 (2006).
- <sup>9</sup>M. Liu, J. Lou, S. D. Li, and N. X. Sun, *Adv. Funct. Mater.* **21**, 2593 (2011).
- <sup>10</sup>M. Liu, S. D. Li, O. Obi, J. Lou, S. Rand, and N. X. Sun, *Appl. Phys. Lett.* **98**, 222509 (2011).
- <sup>11</sup>J. Das, B. A. Kalinikos, and C. E. Patton, *Appl. Phys. Lett.* **91**, 172516 (2007).
- <sup>12</sup>M. Liu, O. Obi, J. Lou, Y. Chen, Z. Cai, S. Stoute, M. Espanol, M. Lew, X. Situ, K. S. Ziemer, V. G. Harris, and N. X. Sun, *Adv. Funct. Mater.* **19**, 1826 (2009).
- <sup>13</sup>Y. Chen, J. Gao, J. Lou, M. Liu, S. D. Yoon, A. L. Geiler, M. Nedoroscik, D. Heiman, N. X. Sun, C. Vittoria, and V. G. Harris, *J. Appl. Phys.* **105**, 07A510 (2009).
- <sup>14</sup>J. Das, Y. Song, and M. Wu, *J. Appl. Phys.* **108**, 043911 (2010).
- <sup>15</sup>J. Lou, M. Liu, D. Reed, Y. H. Ren, and N. X. Sun, *J. Appl. Phys.* **109**, 07D731 (2011).
- <sup>16</sup>N. Li, Y.-H. A. Wang, M. N. Iliev, T. M. Klein, and A. Gupta, *Chem. Vap. Deposition* **17**, 261 (2011).
- <sup>17</sup>W. H. Von Aulock, *Handbook of Microwave Ferrite Materials* (Academic, New York, 1965), pp. 362–379.
- <sup>18</sup>M. I. Bichurin, V. M. Petrov, Yu. V. Kiliba, and G. Srinivasan, *Phys. Rev. B.* **66**, 134404 (2002).
- <sup>19</sup>N. A. Pertsev, H. Kohlstedt, and R. Knöchel, *Phys. Rev. B.* **84**, 014423 (2011).
- <sup>20</sup>A. S. Tatarenko, A. B. Ustinov, G. Srinivasan, V. M. Petrov, and M. I. Bichurin, *J. Appl. Phys.* **108**, 063923 (2010).